

Fluid Velocity Fluctuations in a Suspension of Swimming Protists

Ilia Rushkin^{1,2}, Vasily Kantsler¹ and Raymond E. Goldstein¹

¹*Department of Applied Mathematics and Theoretical Physics, Centre for Mathematical Sciences, University of Cambridge, Wilberforce Road, Cambridge CB3 0WA, UK*

²*School of Mathematical Sciences, University of Nottingham, Nottingham NG7 2RD, UK*

(Dated: August 27, 2018)

In dilute suspensions of swimming microorganisms the local fluid velocity is a random superposition of the flow fields set up by the individual organisms, which in turn have multipole contributions decaying as inverse powers of distance from the organism. Here we show that the conditions under which the central limit theorem guarantees a Gaussian probability distribution function of velocities are satisfied when the leading force singularity is a Stokeslet, but are not when it is any higher multipole. These results are confirmed by numerical studies and by experiments on suspensions of the alga *Volvox carteri*, which show that deviations from Gaussianity arise from near-field effects.

PACS numbers: 87.17.Jj, 47.57.-s, 47.63.Gd, 05.45.-a

A key feature of the inertialess world inhabited by microscopic organisms is the very long-range flow fields they create as they swim. For neutrally-buoyant, self-propelled organisms the far-field behavior of the velocity is that of the force dipole (stresslet) created by the opposed actions of their flagella and cell body on the fluid. Theories incorporating such fields in the fluid stress tensor [1], and simulations of suspensions of dipolar organisms [2] have shown the formation of large coherent structures that are highly suggestive of those seen in experiments on the bacterium *B. subtilis* [3]. The suggestion [3] that hydrodynamic interactions underlie these vortices and jets was made by analogy with the appearance of similar patterns in suspensions of sedimenting particles [4], although interactions in the latter are due to the force *monopole* (Stokeslet) fields arising from the density mismatch between the particles and fluid. Although Stokeslet and stresslet fields have different topologies, it is striking that the two systems display similar coherence.

The relationship between suspensions of microorganisms and of sedimenting particles takes on new significance in light of measurements of velocity fields around freely-swimming organisms [5], which emphasized that the Stokeslet field dominates that of the stresslet beyond a length $\Lambda \sim Td/F_g$, where d is the offset between the flagellar thrust T and the body drag, and F_g is the net gravitational force per organism. Λ can be surprisingly small when compared to the organism radius R : while for the unicellular alga *Chlamydomonas reinhardtii* [6] ($R \sim 5 \mu\text{m}$) $\Lambda \sim 30R$, for its multicellular descendant *Volvox carteri* [7] ($R \sim 200 - 400 \mu\text{m}$) there is the striking conclusion that $\Lambda \sim R$; the Stokeslet dominates the flow field. It was therefore suggested [5] that suspensions of *Volvox* would be more similar to those of sedimenting particles than previously thought, the chief difference being the component of the organism's motion from active swimming. Hence there is fundamental interest in the question: *What are the statistics of fluid velocity fluctuations in a suspension of swimming microorganisms?*

Here we present theory, experiments and simulations that elucidate a number of aspects of this question. We determine the condition on the leading force singularity of a swimmer in order that a random superposition of its velocity field has a Gaussian probability distribution function (PDF). The condition admits the Stokeslet but excludes the stresslet and higher multipoles, so the presence or absence of density matching has a qualitative effect on the statistics. The velocity distribution functions found in experiment and simulation display clear non-Gaussian tails which we suggest arise from near-field effects [8]. The large size of *Volvox* allows study of the scale of fluctuations as a function of the number of organisms at fixed container size, complementary to the limiting procedure often adopted in sedimentation [9]. Our result complement recent studies of the short-time PDFs of tracer particles in suspensions of *Chlamydomonas* [10], where non-Gaussianity was found, and to studies of fluctuations in bacterial baths [11, 12].

Consider a suspension in a box of linear scale L , with N swimmers of radius R . If the volume fraction $\phi = 4\pi R^3 N/3L^3$ is sufficiently small, the PDF of velocities reflects the statistics of a *random* superposition of the flow fields around each swimmer. For a uniform spatial distribution of swimmers, averaging over their positions is equivalent to integrating over space with the swimmer at the origin. If the velocity around a swimmer decays as $|\mathbf{v}(r)| \sim A(\Omega)/r^n$, with Ω standing for angular variables, the probability distribution $P(v)$ of velocities is

$$P(v) \propto L^{-3} \int_0^L \int_{D\Omega} \delta\left(v - \frac{A(\Omega)}{r^n}\right) r^2 dr d\Omega, \quad (1)$$

assuming a spherical container. The tail of the distribution can be determined from the behavior of P under the rescaling $r \rightarrow ar$. Since $\delta(v - A/(ar)^n) = a^n \delta(va^n - A/r^n)$, and noting that for large v the argument of the δ -function vanishes at small r , we deduce that the integral does not depend on the upper limit L/a

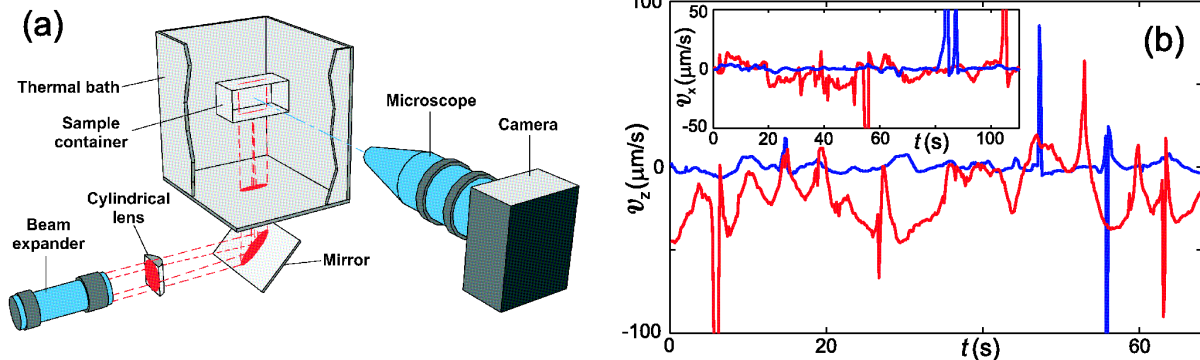


FIG. 1: (color online). Experimental setup and measured velocity fluctuations. (a) Schematic of the imaging and illumination system. (b) Experimental z -component (and x -component, inset) of the fluid velocity in a *Volvox* suspension ($N = 300 \text{ cm}^{-3}$) as a function of time in the central PIV grid domain of the chamber. Red lines indicate velocities in SVM, while blue lines are with approximate density matching of the external fluid: SVM+3% v/v Percoll (Sigma).

(which can be taken to ∞), and hence

$$P(v) = a^{3+n} P(va^n) \rightarrow P(v) \propto \frac{1}{v^{1+3/n}}. \quad (2)$$

The second moment of $P(v)$ is finite only if $n < 3/2$, the case of a Stokeslet ($n = 1$). This is the condition for validity of the central limit theorem; the velocity field from a large number of independently placed Stokeslets is Gaussian. It will not be so for any higher integer singularity, such as stresslets ($n = 2$) or source doublets (here termed ‘sourcelets’) ($n = 3$) [13]. If below a certain radius the decay law deviates from $v \propto r^{-n}$, the PDF shape (2) will break down above the corresponding value of v . Hence, deviations from Gaussianity provide a direct probe of the near-field velocity around the swimmers.

The spherical colonial alga *Volvox* is a remarkably useful system for the study of many aspects of biological fluid dynamics [14–17] because of its size, high symmetry, ease of growth, well-characterized biology, and the existence of a range of mutants. In our experiments, *Volvox carteri f. nagariensis* strain EVE were grown axenically in SVM [18] in a diurnal growth chamber set to a cycle of 16 hours artificial cool daylight ($\sim 4000 \text{ lux}$) at 28°C and 8 h in the dark at 26°C . We used synchronized colonies from the first day of the 48 hour life cycle to obtain the highest motility. A concentration $c = 10 - 500 \text{ cm}^{-3}$ (a volume fraction below $\phi = 0.015$) of organisms was prepared in SVM, with added $2 \mu\text{m}$ polystyrene seeding particles or $6 \mu\text{m}$ tracer particles (Polysciences) at a concentration of $\sim 25 \text{ ppm}$, and placed into a glass container ($1 \times 1 \times 1 \text{ cm}$). The container was placed a thermal bath (Fig. 1a) to eliminate convection [19], and was illuminated with a thin laser sheet ($\lesssim 300 \mu\text{m}$) from a 100 mW, 635 nm laser (BWTEK). Video was captured at frame rates of $0.4 - 5 \text{ Hz}$ by a CCD camera (Pike F145B, Allied Vision Technologies) connected to a long-working distance

microscope (Infinivar CFM-2/S, Infinity Photo-Optical). The fluid velocity was measured by PIV (Dantec Dynamics), typically producing a 63×63 rectangular lattice of velocity vectors. Alternatively, we measured tracer and *Volvox* trajectories by custom (Matlab) PTV software.

Our simulations of protist suspensions used a model in which the velocity field created by a *Volvox* is the sum of a downward-pointing Stokeslet and a sourcelet,

$$\mathbf{v}(\mathbf{r}) = -\frac{3Rv_{\text{sed}}}{4} \left[\left(\frac{\hat{z}}{r} + \frac{(\hat{z} \cdot \mathbf{r})\mathbf{r}}{r^3} \right) + \mu R^2 \left(\frac{\mathbf{n}}{r^3} - \frac{3(\mathbf{n} \cdot \mathbf{r})\mathbf{r}}{r^5} \right) \right],$$

where \mathbf{n} is a unit vector along the colonial axis. The sourcelet represents the near-field flow found by direct measurements [5] and in a model with a constant force density distributed over the colony surface [15], and is important for the statistics of high fluid velocities. Both singularities are cut off at the colony radius. The Stokeslet strength was fixed by an empirical fit to data on the sedimentation velocity as a function of R [16] [$v_{\text{sed}} \simeq \alpha R$, with $\alpha = 1 \text{ s}^{-1}$], while the relative sourcelet strength μ was studied in the range $0 < \mu < 10$. We consider the motion of colonies within a non-interacting ‘ideal gas’ model [20] which, despite its simplicity, gives satisfactory agreement with the experiment; the fluid is unbounded, the swimmers are confined to a rectangular container (cage) with reflecting walls, and the position \mathbf{x}_j of the j th swimmer and its axis vector \mathbf{n}_j evolve as

$$\dot{\mathbf{x}}_j = v_p \mathbf{n}_j + \mathbf{W}_j, \quad \dot{\mathbf{n}}_j = \widetilde{\mathbf{W}}_j, \quad (3)$$

where v_p is the propulsion velocity, \mathbf{W}_j and $\widetilde{\mathbf{W}}_j$ are white noises with diffusion constants D and \widetilde{D} , in 3D and on a unit sphere, respectively. They represent the random influences on the motion of *Volvox* – irregularities of flagellar beating and, partially, mutual advection of colonies.

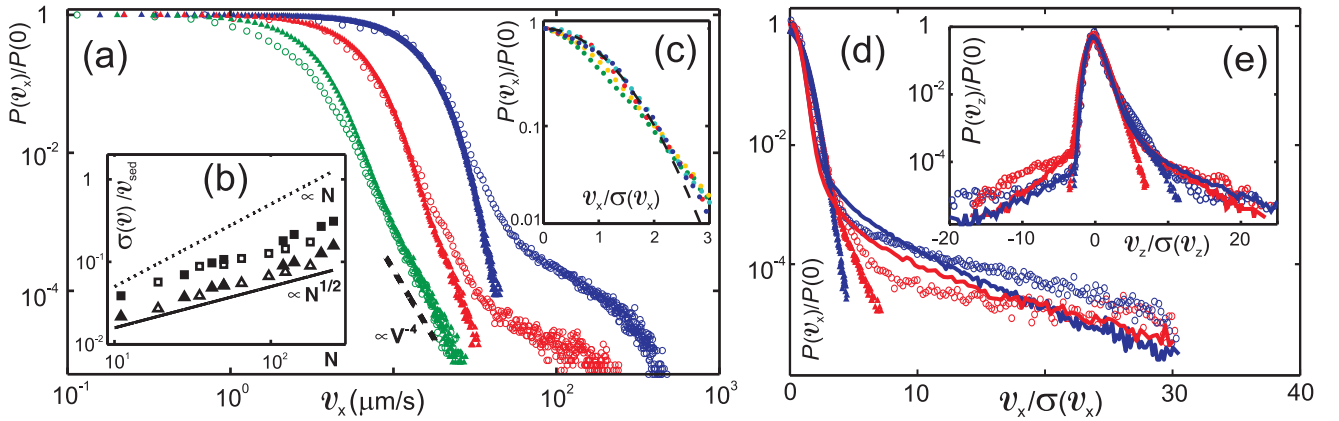


FIG. 2: (color online). Statistics of velocity fluctuations. Colored circles are experimental data for a suspension of *Volvox* with mean diameter $300 \mu\text{m}$. Colored triangles are corresponding numerical simulations excluding sourcelets; solid lines at right are for simulations including sourcelets ($\mu = 4$). Individual colors indicate different numbers of colonies in container: green (11), red (42), and blue (210). (a) PDF of fluctuations in horizontal velocity v_x . (b) Standard deviation of fluid velocity normalized by colony sedimentation speed v_{sed} [z -component (squares), x -component (triangles)], for colony mean diameter $460 \mu\text{m}$ (open symbols), and $220 \mu\text{m}$ (solid symbols). (c) Central region of PDFs of v_x normalized by their standard deviations, for $N = 11, 28, 42, 128$ and 210 . Dashed black line is a Gaussian fit. Full PDFs of (d) v_x and (e) vertical velocity v_z .

The latter is negligible for the most part, since the typical velocity of the resulting flow is found to be much smaller than v_p . This is not true, however, when two or more colonies come close. Although such events are relatively rare, they are important for uniformizing the spatial distribution of *Volvox*: without them the bottom-heavy colonies would gather in the upper part of the container, contrary to observations. For the same reason, including the bottom-heaviness and the sedimentation into (3) in the absence of mutual advection would be inconsistent. The primary (and minor) consequence of neglecting bottom-heaviness is this model does not reproduce the angular distribution of the colonies' axes. Inclusion of sedimentation makes only minor changes to the results.

An example of experimental measurements is the time trace of local fluid velocity in the center of the sample chamber (Fig. 1b). We see that the observed fluid motion is created primarily by the Stokeslets of the swimmers, for when the fluid density was increased to match the density of *Volvox*, the typical velocity fluctuations were reduced drastically. Yet, the peaks due to the near-field source doublets (from a swimmer passing very close to the observation point) remained undiminished.

On a more quantitative level, we examined the PDF of velocity fluctuations (Fig. 2) as a function of the number of colonies in the container, and at various stages in the lifecycle, so that the colony size and sedimentation speed vary over a significant range. Data for the smallest number of swimmers in the container shows a clear power-law tail consistent with the form v^{-4} expected from Eq. 2, and in agreement with simulations done with pure Stokeslets. As expected from a gas of Stokeslets, the PDF of the velocity shows convergence to a Gaussian with the

number of swimmers: for 210 swimmers the Gaussianity persists up to 2.5 standard deviations (Fig. 2c), but with clear tails (discussed below). Once normalized by the sedimentation speed, the standard deviation of the velocity collapses, showing that the fluctuations are proportional to the Stokeslet strength (Fig. 2b). In an ideal gas of Stokeslets, the standard deviation of the velocity fluctuations grows as $\propto \sqrt{N}$ by virtue of the central limit theorem. In the presence of swimmer correlations it should grow faster, but no faster than $\propto N$. The observed law lies between these two powers, much closer to the former (Fig. 2b), supporting the ideal gas approximation, and distinct from the result $N^{1/3}$ found in sedimentation [4], where the mutual advection of particles in each other's Stokeslet fields is the sole contribution to velocity fluctuations. Fluctuations in *Volvox* suspensions are stronger for larger swimmers, due to their larger sedimentation velocity (stronger Stokeslets), and the ratio $\mathcal{R} \equiv \sigma(v_z)/\sigma(v_x)$ is close to 2 for all N . This is found in the numerics with Stokeslets+sourcelets (whose orientations are uniformly distributed). Without sourcelets, the numerics yield $\mathcal{R} \sim 2.8 \approx 2\sqrt{2}$. For a single Stokeslet offset by a sourcelet, the ratio can be computed analytically, averaging over the swimmer's position being replaced by spatial integration, as in (1); \mathcal{R} ranges from 1 (for a randomly directed sourcelet) to $2\sqrt{2}$ for a pure stokeslet.

Inclusion of a sourcelet in the simulations results in tails in the PDFs similar to the experimental data (Fig. 2 right). This allows us to conclude that the observed tails are due to the near-field component of the swimmers' flow. The tails appear to be exponential, but the range of our data is insufficient to prove this. For example, the tail of the data for $N = 210$ is equally well fit by

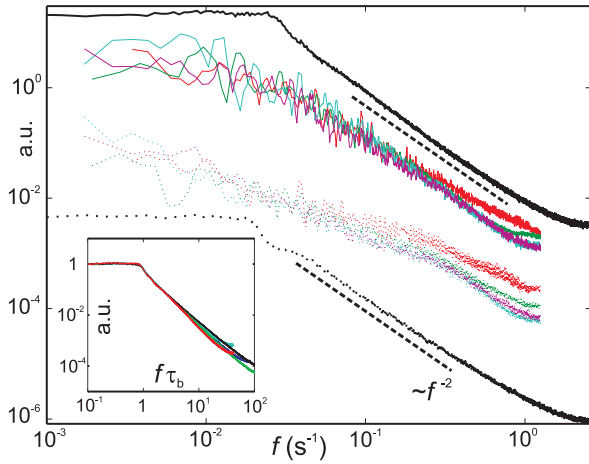


FIG. 3: (color online). Power-spectra of velocities. Solid lines and dotted lines are experimental spectra of v_z and v_x , respectively, for suspensions with mean *Volvox* diameter 290 μm , for $N = 20$ (red), 70 (green), 250 (cyan), and 406 (magenta). Solid and dotted black lines are numerical results for $N = 210$ (rescaled in y), with $\mu = 4$. Inset: collapse of power-spectra in numerics with varying container sizes (0.5-2 cm) and v_p (150-600 $\mu\text{m/s}$), with τ_b from 16.7s to 66.7 s.

$P \propto (v^3 + Nv_*^3)^{-1}$ with $v_* = 25 \mu\text{m/sec}$. A similar situation occurs in the PDF of the vertical velocity, where the core convergence to a Gaussian is less advanced due to the inherent asymmetry of the Stokeslet field.

The velocity power-spectra show a decay close to f^{-2} (Fig. 3), suggesting a Lorentzian power-spectrum of fluctuations $P(f) = (f^2 + (2\pi\tau)^{-2})^{-1}$, i.e. an exponential velocity autocorrelation $\langle \mathbf{v}(0)\mathbf{v}(t) \rangle \propto \exp(-t/\tau)$. Supplemented by the Gaussian PDF, this equation amounts to modeling the velocity fluctuations as an Orstein-Uhlenbeck stochastic process. The motion of *Volvox* is primarily deterministic. For a concentration $c \sim 100 \text{ cm}^{-3}$ the mean free path can be estimated as $(\pi R^2 c)^{-1} \sim 10 \text{ cm}$, which is larger than the container size of $L = 1 \text{ cm}$. Thus, the deterministic term in (3) sets a ballistic time $\tau_b = L/v_p \sim 30 \text{ s}$ which is smaller than the diffusive time scale $\tau_d = L^2/D \sim 100 \text{ s}$ or the dephasing time $\tau_{ph} = 1/\tilde{D} \sim 100 \text{ s}$. Hence, it is τ_b that sets the correlation time in this ideal gas model. We checked it in the numerics (Fig. 3(inset)), and the characteristic τ in the experimental data is close to that in the numerics.

In summary, we have introduced a connection between the statistics of velocity fluctuations in suspensions of swimming protists and the type of force singularity associated with the organism motion. Experiments and numerical results show clearly the existence of non-Gaussianity in the velocity PDFs, which are suggested to arise from the details of fluid flow near the organisms.

The greatest challenge is a theoretical understanding of the form of the non-Gaussianity, which is known to appear as well in other contexts, such as inelastic gases [21].

We are grateful to J.P. Gollub for extensive discussions at an early stage of this work, and thank K. Drescher, K. Leptos, T.J. Pedley, M. Polin, and I. Tuval for advice, and D. Page-Croft, J. Milton, and N. Price for technical assistance. This work was supported by the Schlumberger Chair fund, the BBSRC, the U.S. DOE, Office of Basic Energy Sciences, Division of Materials Science and Engineering, Contract DE AC02-06CH11357, and the European Research Council, Grant 247333.

- [1] R.A. Simha and S. Ramaswamy, Phys. Rev. Lett. **89**, 058101 (2002); D. Saintillan and M.J. Shelley, Phys. Fluids **20**, 123304 (2008); T.J. Pedley, J. Fluid Mech. **647**, 335 (2010).
- [2] J.P. Hernandez-Ortiz, C.G. Stoltz, and M.D. Graham, Phys. Rev. Lett. **95**, 204501 (2005); Saintillan and Shelley, Phys. Rev. Lett. **99**, 058102 (2007).
- [3] C. Dombrowski *et al.*, Phys. Rev. Lett. **93**, 098103 (2004); I. Tuval, *et al.*, Proc. Natl. Acad. Sci. (USA) **102**, 2277 (2005); A. Sokolov, I.S. Aranson, J.O. Kessler, and R.E. Goldstein, Phys. Rev. Lett. **98**, 158102 (2007).
- [4] P.N. Segre, E. Herbolzheimer, and P.M. Chaikin, Phys. Rev. Lett. **79**, 2574 (1997).
- [5] K. Drescher, R.E. Goldstein, N. Michel, M. Polin, and I. Tuval, Phys. Rev. Lett. **105**, in press (2010).
- [6] E. H. Harris, *The Chlamydomonas Sourcebook* (Academic Press, Oxford, 2009), Vol. 1.
- [7] D.L. Kirk, *Volvox* (Cambridge University Press, Cambridge, 1998).
- [8] This conclusion has been arrived at independently: I.M. Zaid, J. Dunkel, and J.M. Yeomans, preprint (2010).
- [9] R.E. Caflisch, J.H.C. Luke, Phys. Fluids. **28**, 759 (1985).
- [10] K. Leptos, *et al.*, Phys. Rev. Lett. **103**, 198103 (2009).
- [11] D.T.N. Chen, *et al.*, Phys. Rev. Lett. **99**, 148302 (2007).
- [12] A. Sokolov, M.M. Apodaca, B.A. Grzybowski, and I.S. Aranson, Proc. Natl. Acad. Sci. (USA) **107**, 969 (2010).
- [13] J.R. Blake and A.T. Chwang, J. Eng. Math. **8**, 23 (1974).
- [14] C.A. Solari, *et al.*, Proc. Natl. Acad. Sci. (USA) **103**, 1353 (2006).
- [15] M.B. Short, *et al.*, Proc. Natl. Acad. Sci. (USA) **103**, 8315 (2006).
- [16] K. Drescher *et al.*, Phys. Rev. Lett. **102**, 168101 (2009).
- [17] K. Drescher, R.E. Goldstein, and I. Tuval, Proc. Natl. Acad. Sci. (USA) **107**, 11171 (2010).
- [18] D.L. Kirk, M.M. Kirk, Dev. Biol. **96**, 493 (1983).
- [19] K. Drescher, K. Leptos, and R.E. Goldstein, Rev. Sci. Instrum. **80**, 014301 (2009).
- [20] T. Ishikawa and T.J. Pedley, J. Fluid Mech. **588**, 437 (2007); T. Ishikawa, J.T. Locsei, and T.J. Pedley, J. Fluid Mech. **615**, 401 (2008).
- [21] F. Rouyer and N. Menon, Phys. Rev. Lett. **85**, 3676 (2000).